

Comprehensive and Definitive Molecular Cytogenetic Characterization of HeLa Cells by Spectral Karyotyping

Merryn Macville,¹ Evelin Schröck, Hesed Padilla-Nash, Catherine Keck, B. Michael Ghadimi,² Drazen Zimonjic, Nicholas Popescu, and Thomas Ried³

Genome Technology Branch, National Human Genome Research Institute [M. M., E. S., H. P.-N., B. M. G., T. R.], and Laboratory of Experimental Carcinogenesis, National Cancer Institute [C. K., D. Z., N. P.], NIH, Bethesda, Maryland 20892

ABSTRACT

We revisited the cytogenetic alterations of the cervical adenocarcinoma cell line HeLa through the use of spectral karyotyping (SKY), comparative genomic hybridization (CGH), and fluorescence *in situ* hybridization (FISH). SKY analysis unequivocally characterized all abnormal chromosomes. Chromosomal breakpoints were primarily assigned by simultaneous assessment of SKY painted chromosomes and inverted 4,6-diamidino-2-phenylindole banding from the same cell. Twenty clonally abnormal chromosomes were found. Comparison with previously reported HeLa G-banding karyotypes revealed a remarkably stable cytogenetic constitution because 18 of 20 markers that were found were present before. The classification of 12 markers was refined in this study. Our assignment of the remaining six markers was consistent with those described in the literature.

The CGH map of chromosomal copy number gains and losses strikingly matched the SKY results and was, in a few instances, decisive for assigning breakpoints. The combined use of molecular cytogenetic methods SKY, CGH, and FISH with site-specific probes, in addition to inverted 4,6-diamidino-2-phenylindole or conventional G-banding analysis, provides the means to fully assess the genomic abnormalities in cancer cells.

Human papillomaviruses (HPVs) are frequently integrated into the cellular DNA in cervical cancers. We mapped by FISH five HPV18 integration sites: three on normal chromosomes 8 at 8q24 and two on derivative chromosomes, der(5)t(5;22;8)(q11;q11q13;q24) and der(22)t(8;22)(q24;q13), which have chromosome 8q24 material. An 8q24 copy number increase was detected by CGH. Dual-color FISH with a *c-MYC* probe mapping to 8q24 revealed colocalization with HPV18 at all integration sites, indicating that dispersion and amplification of the *c-MYC* gene sequences occurred after and was most likely triggered by the viral insertion at a single integration site. Numerical and structural chromosomal aberrations identified by SKY, genomic imbalances detected by CGH, as well as FISH localization of HPV18 integration at the *c-MYC* locus in HeLa cells are common and representative for advanced stage cervical cell carcinomas. The HeLa genome has been remarkably stable after years of continuous cultivation; therefore, the genetic alterations detected may have been present in the primary tumor and reflect events that are relevant to the development of cervical cancer.

INTRODUCTION

HeLa was derived from an adenocarcinoma of the cervix in 1952 and was the first human epithelial cancer cell line established in long-term culture (1). The cells have a hypertriploid chromosome number (3n+), specific numerical deviations, 20 clonally abnormal chromosomes [known as HeLa signature chromosomes or HeLa

markers (2)], and contain multiple copies of the HPV⁴ type 18 (HPV18), integrated at specific sites (3). These are stable characteristics following numerous years of weekly subculturing and provide a diagnostic tool for the detection of cross-contamination of cell cultures with HeLa cells.

HeLa cells have been used in a broad variety of investigations, including the identification of chromosomes and genes in somatic cell hybrids controlling the tumorigenicity in cervical carcinoma (4, 5). Because of the wide interest in this cell line, there has been a considerable effort over the years by experienced cytogeneticists to characterize in detail the chromosomes of HeLa and derivative lines. Thus far, G-banding and FISH with chromosome painting probes (2, 4, 6–12) have been the staining techniques of choice, but both methods have their limitations. Classical cytogenetic analysis of solid tumor cell lines often remained incomplete, because chromosome regions that appeared abnormal did not always have a characteristic band that could be accurately identified, and, in addition, the high number of aberrations impeded a characterization of all abnormal chromosomes. FISH with chromosome painting probes was mostly used as a confirmatory technique that required previous knowledge of cytogenetic abnormalities. Whole-genome analysis is time-consuming because it requires iterative experiments with different probes (12). Now these methodological limitations can be overcome by 24-color FISH for the differential visualization of all 24 chromosomes in one experiment (13, 14).

Here, we applied advanced molecular cytogenetic techniques to the analysis of HeLa chromosomes and provided its complete and definitive cytogenetic profile. The data were generated by SKY (14, 15), concomitant inverted DAPI banding analysis, CGH for detecting changes in DNA copy number throughout the tumor genome (16), and conventional FISH to verify the composition of complex marker chromosomes.

MATERIALS AND METHODS

HeLa Metaphase Preparation. HeLa CCL2 cells were obtained at passage 90–102 from American Type Culture Collection (Rockville, MD) and have been stored in liquid nitrogen stocks. The same stocks were used before for G-banding karyotype analysis (6) and isotopic *in situ* hybridization for chromosome localization of HPV18 integration sites (3). HeLa metaphase specimens were prepared according to standard cytogenetic procedures for solid tumors (17).

SKY. SKY is based on FISH, epifluorescence light microscopy, digital imaging, and Fourier transform spectroscopy (16). The SKY hybridization protocol has been described in detail (14, 18). Essentially, metaphase cells of HeLa were pretreated and hybridized with a SKY probe mixture containing 24 uniquely labeled chromosome-specific probes. Probes were obtained by high-resolution flow sorting, amplified by two consecutive rounds of degenerate oligo-primed (DOP)-PCR amplification (19), and were subsequently combinatorially labeled with three fluorochromes and two haptens to create a unique spectral signature for every chromosome. We used the fluorochromes Spec-

Received 6/25/98; accepted 10/29/98.

The costs of publication of this article were defrayed in part by the payment of page charges. This article must therefore be hereby marked *advertisement* in accordance with 18 U.S.C. Section 1734 solely to indicate this fact.

¹ Present address: Laboratory for In Situ Hybridization, Institute of Pathology, University of Nijmegen, P. O. Box 9101, 6500 HB Nijmegen, the Netherlands. E-mail: m.macville@pathol.azn.nl.

² Received a fellowship from the Deutsche Krebshilfe.

³ To whom requests for reprints should be addressed, at Genome Technology Branch, National Human Genome Research Institute, NIH Building 49, Room 4A28, 49 Convent Drive, Bethesda, MD 20892-4479. Phone: (301) 594-3118; Fax: (301) 435-4428; E-mail: tried@nhgri.nih.gov.

⁴ The abbreviations used are: HPV, human papillomavirus; FISH, fluorescence *in situ* hybridization; SKY, spectral karyotyping; DAPI, 4,6-diamidino-2-phenylindole; CGH, comparative genomic hybridization; TRITC, tetramethylrhodamine isothiocyanate.

trum Green, Spectrum Orange (dUTP conjugates; Vysis, Downers Grove, IL) and Texas Red (12-dUTP conjugate; Molecular Probes, Eugene, OR) for direct labeling and biotin-16-dUTP and digoxigenin-11-dUTP (Boehringer Mannheim, Indianapolis, IN) for indirect labeling. After hybridization, biotin was detected with Avidin~Cy5 (Vector, Burlingame, VT), and digoxigenin-11-dUTP with mouse anti-digoxin (Sigma Chemical Co., St. Louis, MO), followed by sheep anti-mouse custom-conjugated to Cy5.5 (Amersham Life Sciences, Arlington Heights, IL). The slides were counterstained with DAPI and covered in *para*-phenylene-diamine antifade solution (Sigma).

Spectral images were captured with a SD200 SpectraCube system (Applied Spectral Imaging, Migdal Ha'Emek, Israel) mounted on a Leica DMRBE microscope (Leica, Wetzlar, Germany). Samples were illuminated with a 150 W Xenon lamp (Opti Quip, Highland Mills, NY) and imaged with a 63x/ N.A.1.25 plan apo oil immersion objective (Leica) through a custom-designed triple bandpass optical filter (SKY v.3; Chroma Technology, Brattleboro, VT). Fourier transformation recovers the spectrum from this interferogram (16, 20). Spectrum-based classification of the raw spectral images is performed using SkyView 1.2 software (Applied Spectral Imaging). The visualization software applies an RGB look-up table to the raw spectral image resulting in the infra-red emission being displayed in red, red emission in green, and green emission in blue. The display image is a true representation of the SKY hybridization because it is based on the fluorescence intensities of all chromosome painting probes (Fig. 1A). A mathematical classification algorithm is applied to unambiguously discriminate differentially labeled chromosomes based on their emission spectrum (16) and assigns to each pixel in the image with the same emission spectrum the same classification (pseudo-) color (Fig. 1, B and D). DAPI banding gray-scale images of the same cells were captured separately, electronically inverted, and contrast-enhanced in SkyView 1.2 (Applied Spectral Imaging; Fig. 1C). To define chromosomal breakpoints, the high-quality inverted DAPI banding images were aligned with the SKY classified chromosomes. Cytogenetic nomenclature adheres to ISCN (21) standards based on G-banding at the 400 band level.

Karyotype Comparison. To objectively compare our HeLa karyotype to karyotypes published previously, figures from the original papers (2, 4, 6–12) were digitally scanned, and images were normalized for size and black and white levels using Adobe Photoshop 3.0. Fig. 1E is based on the G-banding karyotype of HeLa cells published previously (6). The HeLa cells used for SKY and inverted DAPI banding analysis in the present study are from the same clone and passage, and metaphase slides have been prepared under the same culturing conditions.

CGH. CGH was performed on blood lymphocyte metaphases from a healthy female donor. Whole genomic DNA was extracted from blood lymphocytes and HeLa cells according to standard procedures (22). CGH procedures have been described in detail previously (23). In short, control and test genomes were differentially labeled by nick translation with, respectively, digoxigenin-11-dUTP and biotin-16-dUTP (Boehringer-Mannheim). Co-hybridization with centromere-specific probes (24) for chromosomes 4, 8, 14, 20, 22, and X greatly facilitates chromosome classification critical for proper evaluation of CGH results. Hybridization of pretreated metaphase slides was performed for two nights at 37°C in a humidified chamber. Immunocytochemical detection of haptenized probes have been described previously (25). Chromosomes were counterstained with DAPI and covered in *para*-phenylene-diamine (Sigma) antifade solution. For image acquisition, we used Leica QFISH software (Leica Imaging Systems, Cambridge, United Kingdom) interfaced to a cooled CCD camera (CH250; Photometrics, Tucson, AZ) and a Leica DMRXA microscope that was especially equipped for CGH image capture with four aligned optical filters for DAPI, FITC, TRITC, and Cy5 (TR1, TR2, TR3, and 41008; Chroma Technology). CGH ratio profiles were calculated on a Cytovision 3.0 workstation (Applied Imaging, Cambridge, UK) that was custom-upgraded for the display of the fourth image showing the Cy5 centromere ISH signals. The average ratio profile was calculated as a mean value of 15 metaphase spreads. Detection thresholds were 0.75 for copy number losses and 1.25 for copy number gains.

FISH. To verify the composition of complex marker chromosomes, dual-color FISH was performed with painting probes for chromosomes 8 and 22 (M6, M16), chromosomes 7 and 19 (M8), and chromosomes 9 and 11 (M11), allegedly present in the markers. Chromosome preparations obtained from exponentially growing HeLa cells were hybridized with a HPV18 probe cloned from a cervical carcinoma biopsy used previously for isotopic *in situ* hybrid-

ization mapping of the virus in HeLa chromosomes (3), genomic probes for *c-MYC* and *c-ABL1* genes (Oncor, Gaithersburg, MD), and YAC 850A and a cosmid probe specific for region 3p14.2 [kindly provided by Dr. Kay Huebner (26, 27)]. FISH probes were labeled with biotin or digoxigenin by random priming (Boehringer-Mannheim) and visualized by FITC and TRITC, respectively. The conditions for FISH, digital image acquisition, processing, and analysis were performed as described previously (27, 28).

RESULTS

Molecular cytogenetic analysis of HeLa cells was performed by SKY, CGH, and FISH. SKY analysis always included inverted DAPI banding assessment of the same cell. The spectral images of a representative cell (A1) are shown in Fig. 1, A–D, and the SKY results from six fully analyzed HeLa cells are presented in Table 1. A combined map of chromosomal gains and losses as detected with SKY and CGH is depicted in Fig. 2. Both SKY and CGH contributed to the elucidation of the karyotype as demonstrated in Table 2, classifying all chromosomal regions and breakpoints in rearranged chromosomes. The definitive HeLa karyotype is compared with karyotypes published previously (Table 3) to demonstrate the stability of this cell line over the years with respect to the presence of the numerous markers. Furthermore, FISH with gene-specific probes demonstrated colocalization of HPV18 with *c-MYC* on two marker chromosomes, M6 and M16 (Fig. 3A).

SKY. SKY analysis of HeLa cells generated a complete karyotype, leaving no markers of unknown origin (Fig. 1, A–D). The SKY results are based on 24 HeLa metaphase cells, 6 of which are fully described (Table 1). The remaining spreads were either incomplete or contained too many overlaps and were used primarily to confirm the presence of recurring aberrations. HeLa cells are hypertriploid (3n+) containing a total number of 76–80 chromosomes and 22–25 abnormal chromosomes per cell. Two subclones were identified. Subclone A contains 18 abnormal chromosomes, M1 to M16, M19, and M20, and subclone B was defined by two additional abnormal chromosomes, M17 and M18. M19 and M20 were never found together in the same cell and occurred in both subclones A and B. The markers M1 t(1q;3q), M2 t(1p;9q), M10 t(3p;9p) are involved in a complex balanced translocation.

Gray-scale images of the DAPI counterstain from the same cells were electronically inverted (Fig. 1C) and aligned with the spectrally analyzed chromosomes to define the chromosomal breakpoints. Common chromosomal breakpoints in subclones A and B were localized at 9 centromeric regions, 1p10, 3p10, 3q10, 5p10, 5q10, 9p10, 13q10, 15q10, and 20q10, and at 25 chromosome bands, 1q11, 2q31*, 2q36*, 3p11, 3q11, 3q21, 5q11, 7p21, 7q35, 8q24*, 9p11, 9q34*, 11p11*, 11p14*, 11q13*, 11q22*, 12q15, 13q12, 13q14, 13q21, 16p11, 19p13*, 19q11, 22q11, and 22q13. In some cases, we were not able to determine the exact chromosomal breakpoints by SKY and inverted DAPI banding alone. However, in cases where a recurrent aberration resulted in a genetic copy number change, the CGH ratio profile was indicative for the breakpoints. The breakpoints marked with an asterisk denote those that were identified using CGH (Table 2). Several of these regions are involved in recurrent aberrations associated with cervical cancer and other malignancies.

CGH. CGH is a single-experiment screening test used to map gains and losses in a tumor genome and to localize potential sites of proto-oncogenes and tumor suppressor genes. The average ratio profile in Fig. 2 shows the chromosomal regions in HeLa with a decreased or increased copy number (see the figure legend for details). We found copy number gains of chromosome 1, chromosome arms 5p, 9p, 15q, 16p, and 20q, and regions 2q31→q36, 3pter→p21, 5q11→q32, 7pter→q35, 8q24→qter, 9q34→qter, 11p14→p11,

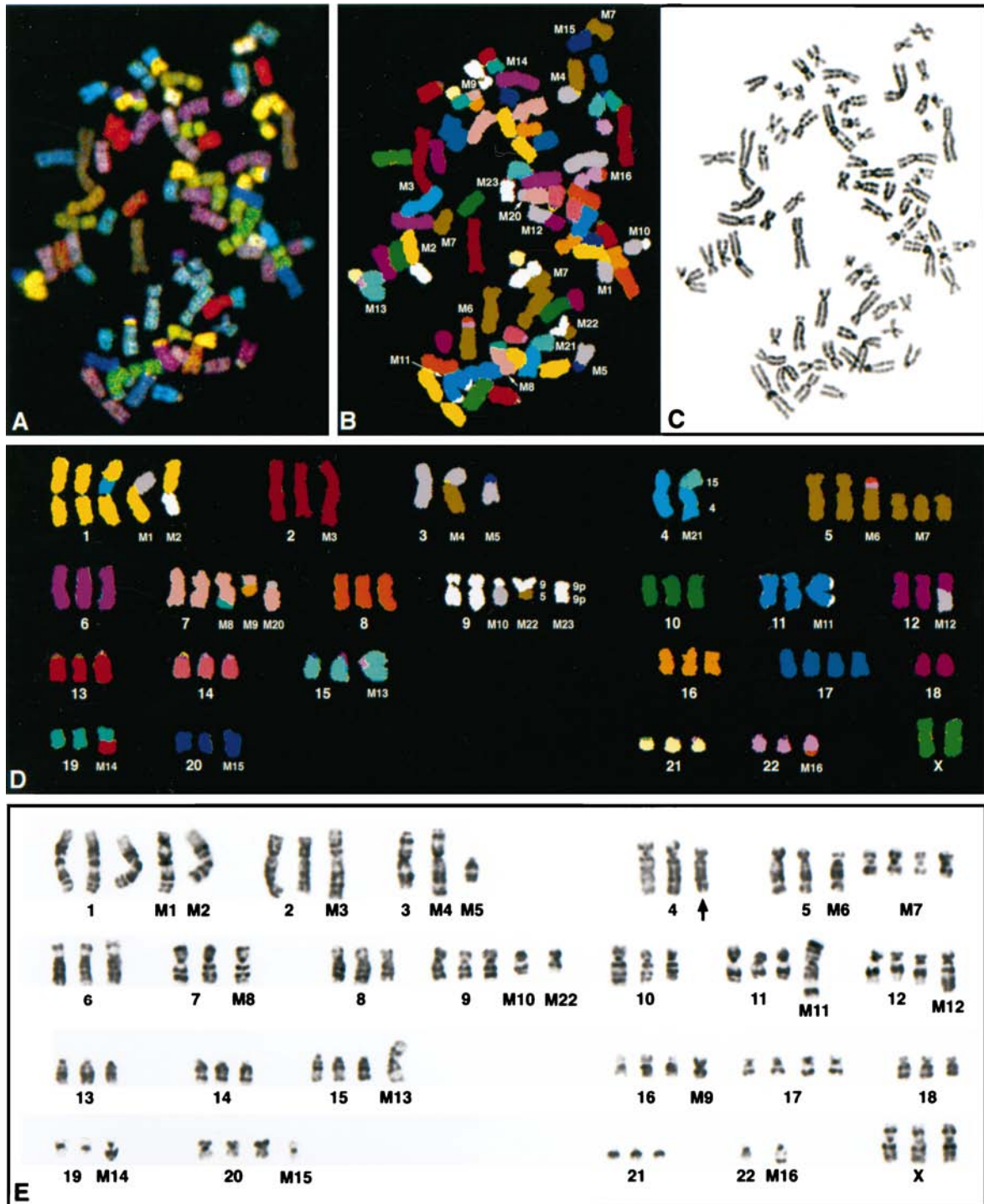


Fig. 1. A, an RGB display of the 24-color SKY hybridization of a representative HeLa metaphase from subclone A (cell A1). The same metaphase in SKY classification colors (B), in gray-scale inverted DAPI banding (C), and arranged in a SKY karyotype (D) is shown. E, a previously published G-banding karyotype of HeLa from the same clone and passage as has been used for SKY analysis [figure used with permission, Popescu *et al.* (6)] and has been adjusted according to SKY results. Arrow, a possible deletion of 4q32→qter as detected by CGH but not by SKY.

11q13→q22, and 12pter→q15. Copy number losses were detected for chromosome arm 20p and regions 4q32→qter, 7q35→qter, 11q23→qter, and 13q10→q14 (Table 2).

HeLa Karyotype. The results of SKY, CGH, and FISH analyses of HeLa cells are combined and described in detail in the following section. CGH was primarily used to complement SKY. From SKY and previous cytogenetic studies, HeLa was found to be a hypertriploid cell line ($3n+$). Therefore, CGH detected copy number gains for

chromosome regions if they were present in more than three copies in the majority of cells and mapped copy number losses for regions if they occurred in fewer than three copies. Fig. 2 depicts the combined SKY and CGH results aligned next to their respective chromosome ideograms. SKY amplification-deletion is depicted as a color bar on the left side of the chromosome ideograms, and CGH gains and losses are shown as average ratio profiles on the right side of each chromosome ideogram (see the figure legend for details). Table 2 summarizes

Table 1 Number of copies of chromosomes of six HeLa cells analyzed by SKY and inverted DAPI banding

HeLa karyotype is based on SKY analysis of 24 metaphase cells. Six cells were fully analyzed and listed here. Two subclones A and B were characterized. The clonally aberrant chromosomes M1 to M20 are highlighted in bold, and the subclone B-specific markers M17 and M18 are in italics. Some breakpoints could not be determined without CGH data and are, therefore, left open or question marked.

Subclone	A			B			
	Cell	A1	A2	A3	B1	B2	B3
Chromosome							
1		3	3	2	3	3	3
2		2	2	2	2	2	2
3		1	1	1	1	1	1
4		1	3	3	3	3	3
5		2	2	2	2	2	2
6		3	3	3	3	3	3
7		2	1	2	3	3	2
8		3	3	3	3	3	3
9		2	2	1	2	3	1
10		3	3	3	3	3	3
11		2	2	2	2	2	3
12		2	3	3	3	2	3
13		3	2	2	0	2	1
14		3	3	3	3	3	3
15		2	3	1	2	2	2
16		3	3	3	3	3	3
17		4	3	4	4	4	4
18		2	3	3	2	3	3
19		2	2	2	2	2	2
20		2	2	2	2	2	2
21		3	3	2	2	2	2
22		2	1	2	2	2	2
X		2	3	2	3	3	3
Marker							
M1 der(1)t(1;3)(q11;q11)		1	1	1	1	1	1
M2 der(1;9)(p10;q10)		1	0	1	1	1	1
M3 dup(2)(q?q?)		1	1	1	1	1	1
M4 der(3;5)(p10;q10)		1	1	1	1	1	1
M5 der(3;20)(q10;q?10)		1	1	1	1	1	1
M6 der(5)t(5;22;8)(q11;q11q13;?)		1	1	1	1	1	1
M7 i(5)(p10)		3	5	4	4	4	3
M8 der(7)t(7;19)(q35;?)		1	1	1	1	1	1
M9 der(16)t(7;16)(p21;p11)		1	1	1	1	1	1
M10 der(9)t(3;9)(p21;p11)		1	1	1	1	1	1
M11 der(11)t(9;11;9)(?;p14;q22;?)dup(11)(p?)dup(11)(q?)		1	1	1	1	1	1
M12 der(12)t(3;12)(q21;q15)		1	1	1	1	1	1
M13 i(15)(q10)		1	1	1	1	1	1
M14 der(19)t(13;19)(q21;p13)		1	1	1	1	1	2
M15 i(20)(q10)		1	1	1	1	1	1
M16 der(22)t(8;22)(?:q13)		1	1	1	1	1	1
<i>M17</i> der(13;13)(q10;q10)del(13)(q12)del(13)(q14)		0	0	0	1	1	1
<i>M18</i> der(15;21)(q10;q10)		0	0	0	1	1	1
M19 del(7)(p21)		0	2	1	0	1	1
M20 der(7)t(3;7)(?:p21)		1	0	0	1	0	0
M21 der(4;15)(q10;q10)		1	0	0	0	0	0
M22 der(5;9)(p10;p10)		1	0	0	0	0	0
M23 i(9)(p10)		1	0	0	0	0	0
M24 17ps		0	1	0	0	0	0
M25 der(1;21)(q10;q10)		0	0	1	0	0	0
M26 der(3)t(3;9)(q25;q34?)del(3)(p21?)		0	0	1	0	0	0
M27 der(5;5)(p10;p10)t(5;22)(p15;q13?)		0	0	1	0	0	0
M28 del(13)(q13)		0	0	1	0	0	0
M29 der(13;19)(q10;p10)		0	0	0	1	0	0
M30 18ps		0	0	0	1	0	0
M31 i(20)(p10)		0	0	0	1	0	0
m ^a		22	22	24	25	22	22
N		76	78	77	80	80	78

^a m, total number of markers listed per cell; N, total number of chromosomes per cell.

the number of normal chromosomes present, the regions present in the markers, and the total sum of chromosomal material for chromosomes 1–22 and the X as assessed by SKY and inverted DAPI banding analysis. Furthermore, Table 2 lists the gains and losses as detected by CGH and additional FISH data verifying and refining the SKY results. The definitive karyotype resulting from the combined SKY, inverted DAPI banding, and CGH and FISH analyses is given in Table 3.

HeLa contained three normal chromosomes 1 and two clonal markers, M1 der(1)t(1;3)(q11;q11.2) and M2 der(1;9)(p10;q10), resulting in tetraploidy for chromosome 1. In Fig. 2, the green bar left of the idiogram represents the extra chromosome 1 material in M1 and M2 as detected by SKY. This was in concordance with the CGH average

ratio profile for chromosome 1 showing a gain for both the p and q arms.

There were two normal chromosomes 2 present and one clonal marker (M3) that had an elongated 2q arm. SKY and inverted DAPI banding could not determine which region of chromosome 2 was amplified because of its undefined chromosomal banding pattern. CGH, however, suggested a duplication of 2q31→q36. In Fig. 2, this region is indicated by a green dotted bar.

Chromosome 3 had one normal copy and was involved in six clonal markers (M1, M4, M5, M10, M12, and M20). M1 and M5 were whole-arm translocations both containing 3q, producing a triploid copy number for 3q. M4 and M10 both contained the whole p arm,

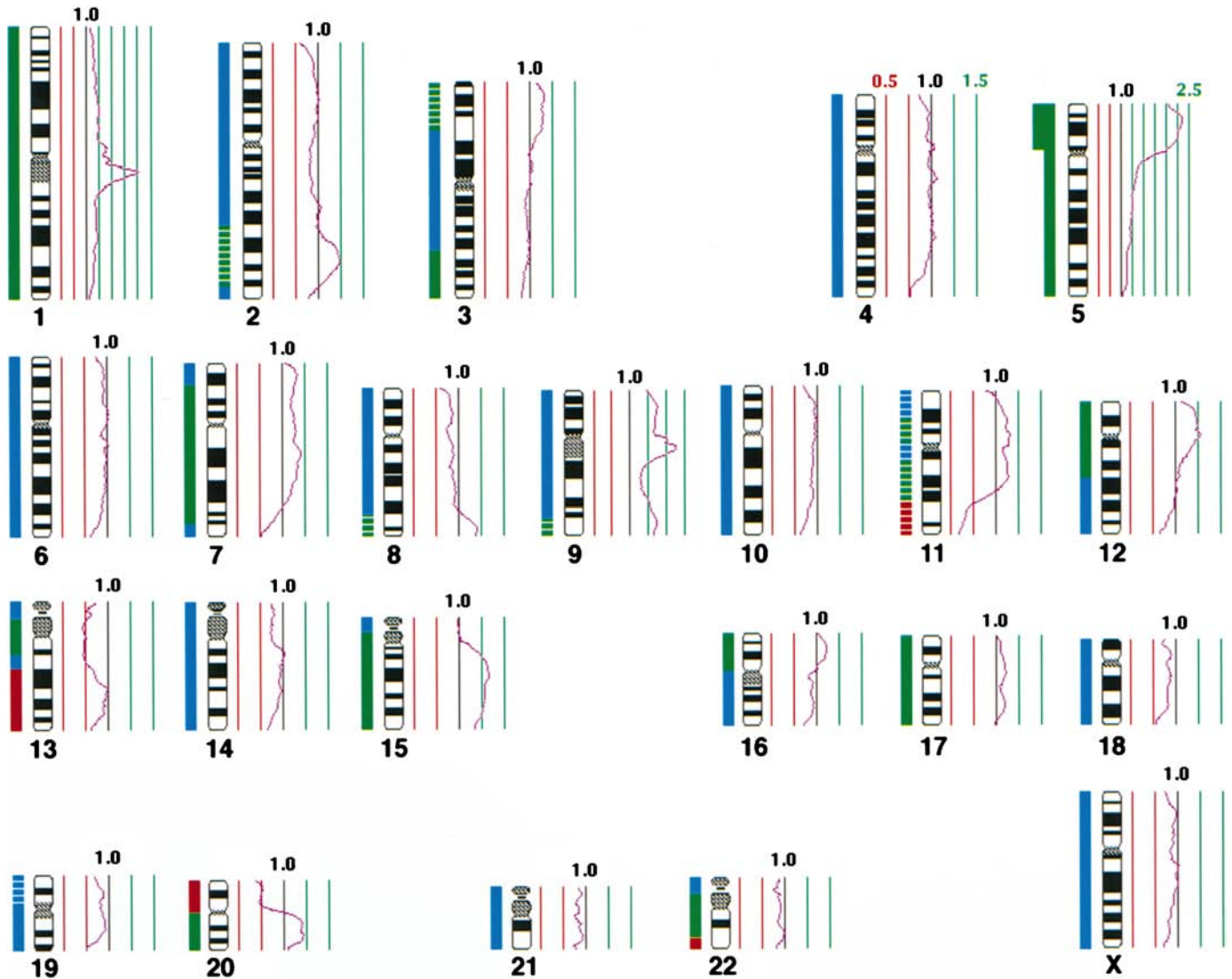


Fig. 2. Chromosome ideograms with SKY amplification-deletion map (left of ideogram) and CGH ratio profile (right of ideogram). The SKY amplification-deletion map is based on 24 cells and is depicted as a color bar in which green indicates amplified regions, blue indicates modal ($3n$) regions, and red indicates deleted regions. Thick green bars, multiple amplified regions. Dotted bars, regions that were assigned with the help of CGH. Right, CGH average ratio profile; vertical lines, different values of the fluorescence ratio between tumor and normal reference DNA. The black middle line ($r = 1.0$) marks the balanced situation, the first red line on the left ($r = 0.75$) marks the threshold for copy number losses, and the first green line on the right ($r = 1.25$) marks the threshold for copy number gains. Note the remarkable consistency between the SKY amplification-deletion map and the map for CGH gains and losses.

adding up to a triploid copy number for 3p as well. M12 possibly contained 3q21→qter, resulting in one copy gain for this region. CGH showed a balance for 3p14→qter and gain of 3p21→pter, suggesting that 3p21→pter was present in marker 20. FISH with a cosmid probe spanning the FRA3B/FHIT locus at 3p14.2 demonstrated hybridization signals for the probe on the normal copy of 3, M4, and M10 but not on M20 (Fig. 3B).

Chromosome 4 usually had three normal copies. CGH suggested a loss of 4q32→qter, whereas SKY and inverted DAPI banding did not show the deletion. In the Giemsa-stained karyotype (Fig. 1E), there was one chromosome 4 (arrow) that appeared shorter and may have a small deletion. Additional high-resolution G-banding or FISH analysis with 4q telomere-specific probes would perhaps resolve this discrepancy.

Two normal chromosomes 5 were present in HeLa in addition to three clonal markers (M4, M6, and M7). M4 and M6 each contained the whole 5q arm, including the centromere, resulting in a gain of 5q material. M7 was an isochromosome 5p and was present in three to five copies. Furthermore, some cells had nonclonal markers that

contained 5p (M22 and M27). We have detected up to 12 copies of 5p in one cell. CGH revealed a gain of 5q and a high copy number gain of 5p.

HeLa usually contained two normal chromosomes 7, two clonal markers (M8 and M9), and two markers present in subclones A and B that are mutually exclusive (M19 and M20). M8 is a der(7)t(7;19) with 7pter→7q35 present. M9 contained part of 7p, possibly 7pter→p21, translocated to 16p. M19 and M20 are derivatives 7, both containing 7p21→qter. Chromosome 7 material in these markers was confirmed by conventional FISH. In total, the SKY amplification-deletion map showed a gain for 7pter→7q35 and a balance for 7q35→qter. This was partly reflected in CGH, which showed a gain of 7pter→7q35 and a loss for 7q35→qter. The loss of 7q35→qter was perhaps due to the presence of subpopulations of HeLa containing fewer than two normal chromosomes 7.

Chromosome 8 was represented by three normal copies and two clonal markers (M6 and M16). In a previous study, the markers M6 and M16 were found to contain HPV18 sequences, but their origin could not be elucidated by G-banding (3). SKY revealed a piece of

Table 2 Combined results of SKY, inverted DAPI banding, CGH, and FISH analyses

Listed are the number of normal chromosomes commonly present, marker number(s) involving the chromosome, the regions present in the marker(s) as determined by SKY, and the amplified or deleted regions relative to the triploid cell number. The regions gained and lost as detected by CGH are listed as well as additional FISH results.

Chromosome	SKY		Region present in marker	Amplification and deletion (3n)	CGH gains & losses	FISH
	No. of normal copies	Marker				
1	3	M1 M2	1q11→qter 1p10→ppter	+1p +1q	+1	
2	2	M3	dup(2q?)	+2q?	+2q31→q36	
3	1	M1 M4 M5 M10 M12 M20 ^a	3q11→qter 3p10→ppter 3q10→qter 3p11→ppter 3q21→qter 3p?	+3q21→qter +3p?	+3pter→p21	YAC 850A (3p14.2) on M4, M10
4	3			Balanced	-4q32→qter	
5	2	M4 M6 M7	5q10→qter 5q11→qter 5p10→ppter ×6-10	+ +5p +5q	+ +5p +5q11→q32	
6	3			Balanced	Balanced	
7	2	M8 M9 M19 ^a M20 ^a	7pter→7q35 7p21→ppter? 7p21→7qter 7p21→7qter	+7pter→q35	+7pter→q35, -7q35→qter	Chromosome 7 confirmed
8	3	M6 M16	8q? 8q?	+8q?	+8q24→qter	Chromosome 8 confirmed, c-MYC (8q24) on M6, M16
9	2	M2 M10 M11	9q10→qter 9p11→ppter 9q?	+9q?	+9p +9q34→qter	Chromosome 9 confirmed, c-ABL1 (9q34) on M2, M11
10	3			Balanced	Balanced	
11	2	M11	11p14?→11q22? dup(11p?) dup(11q?)	+11p?, +11q? -11pter→p15? -11q23→qter?	+11p14→p11 +11q13→q22 -11q23→qter	Chromosome 11 confirmed
12	3	M12	12pter→q15	+12pter→q15	+12pter→q15	
13	2	M14 M17 ^b	13q21→qter 13q10→q12 13q10→q14	-13q10→q14	-13q10→q14	
14	3			Balanced	Balanced	
15	2	M13 M18 ^b	15q10→qter ×2 15q10→qter	+15q	+15q	
16	3	M9	16p10→ppter	+16p	+16p	
17	4			+17	Balanced	
18	3			Balanced	Balanced	
19	2	M8 M14	19p? 19p13→qter	Balanced? Balanced?	Balanced	Chromosome 19 confirmed
20	2	M5 M15	20q10→qter 20q10→qter ×2	-20p +20q	-20p +20q	
21	3	M18 ^b	21q10→qter	Balanced	Balanced	
22	2	M6 M16	22q11→q13 22q11→q13	+22q11→q13 -22q13→qter	Balanced	Chromosome 22 confirmed
X	3			Balanced	Balanced	

^a Markers M19 and M20 are mutually exclusive and occur in subclones A and B.

^b M17 and M18 are subclone B-specific markers and are present in 50% of the cells.

chromosome 8 at the telomeric ends, which was confirmed by conventional FISH (data not shown), although the exact banding region could not be determined by this method. However, CGH indicated a gain of 8q24→qter, the site of the *c-MYC* proto-oncogene, suggesting there were extra copies of the *c-MYC* gene. Remarkably, dual-color FISH with HPV18 and *c-MYC*-specific probes revealed 100% colocalization on normal chromosome 8 and on M6 and M16, verifying that 8q24 was present in both markers (Fig. 3A).

Chromosome 9 was usually represented by two normals and three clonal markers (M2, M10, and M11). M2 contained 9q, and M10 contained 9p, including the centromere, hereby balancing chromosome 9 material. Conventional FISH with chromosome 9 and *c-ABL1* probes has confirmed the presence of chromosome 9 material at both distal ends of M11 and detected the presence of five copies of the *c-ABL1* gene (data not shown). CGH showed a distinct gain of 9q34→qter. SKY identified two nonclonal markers containing the 9p arm (M22 and M23). It is conceivable that HeLa is heterogeneous with regards to 9p markers because CGH showed a gain for 9p.

HeLa had two normal copies of chromosome 11 and one clonal marker (M11) containing a complex intrachromosomal rearrangement that remained elusive after inverted DAPI and G-banding analysis.

CGH indicated amplification of 11p14→p11 and 11q13→q22 and loss of 11q23→qter.

The average number of normal chromosomes 12 was three. One clonal marker (M12) contained 12pter→q15, thereby resulting in an overall gain for this region. Accordingly, CGH showed an increased copy number for 12pter→q15 and was balanced for 12q15→qter.

Chromosome 13 was present as two normal copies in subclone A and ranged from zero to two normals in subclone B. Marker M14 contained 13q21→qter and was present in both subclones. M17, an isochromosome 13q with deletions in both arms at 13q12 and 13q14, respectively, is subclone B specific. On the basis of the SKY analysis of subclone A alone, one would expect a loss for 13q10→q21 and a balance for 13q21→qter, as shown by CGH. The contribution of chromosome 13 material from subclone B-specific marker M17 did not balance the region 13q10→q14, because subclone B often showed concomitant loss of normal chromosomes 13.

Chromosome 15 was present in two normal copies, one clonal marker isochromosome 15q (M13), and one subclone B-specific marker also containing 15q (M18), contributing to four or five copies/cell. CGH showed a gain of 15q.

HeLa cells always contained three normal chromosomes 16 and one

Table 3 *Marker assignment in previously published HeLa karyotypes of the abnormal HeLa chromosomes defined in this study*

The descriptions of HeLa markers as found by comprehensive molecular cytogenetic analysis in this study are listed as M1 to M31 in column a. Denotation in bold indicates the markers that were newly described in this study. Columns b to k contain the corresponding annotation of the markers in previous G-banding karyotypes of HeLa CCL2 (b,c,d,e,f, and g), HeLa S3 (c and g), and HeLa D98/AH2 (e,h, and i) and one FISH study of D98/AH2 (j) from the literature: b, Popescu and DiPaolo (6); c, Chen (2); d, Mincheva *et al.* (7); e, Heneen (8); f, Kraemer *et al.* (9); g, Nelson-Rees *et al.* (10); h, Francke *et al.* (11); i, Stanbridge *et al.* (4); and j, Ruess *et al.* (12). Listing in italics indicates a marker described in the same way as we did. A question mark indicates a reason for doubt whether the marker was present.

Marker	HeLa CCL2							HeLa S3		D98/AH2			
	a	b	c	d	e	f	g	c	g	e	h	i	j
der(1)t(1;3)(q11;q11)	M1	<i>m2</i>	<i>m1</i>	m1	<i>m5</i>	mA	m1	<i>m1</i>	m1				
der(1;9)(p10;q10)	M2	1c	<i>m2</i>	m11	m3?	mB?	m6	<i>m2</i>					
dup(2)(q31;q36)	M3	2b	m3	m8	m12	2b?							
der(3;5)(p10;q10)	M4	<i>m1</i>	<i>m4</i>	m2	m2	mD	m2	<i>m4</i>	m2	m1	m1	m3	<i>m1</i>
der(3;20)(q10;q10)	M5	13a?	m5	m15	m21	mH	m5	m5					
der(5)t(5;22;8)(q11;q11q13;q24)	M6	m6	m6	5b	5a	5a?			m14				
i(5)(p10)	M7	<i>m8</i>	<i>m7</i>	m5	<i>m10</i>	mN	m3			m2	m8	m6	<i>m11</i>
der(7)t(7;19)(q35;p13)	M8	7b			7?	7							
der(16)t(7;16)(p21;p10)	M9	m9a	m12?	m7?	20c?	mR?							
der(9)t(3;9)(p11;p11)	M10	11b		m14	m15	mE							
der(11)t(9;11;9)(q34;p14q22;q34)dup(11)(p11p14)dup(11)(q13q22)	M11	m3	m19	m10	m13	UCa		m19	m11				
der(12)t(3;12)(q21;q15)	M12	m5	m15	m13	m19	mI		m25		m7	m4	m15	<i>m6</i>
i(15)(q10)	M13	<i>m4</i>	<i>m17</i>	m3	M8								
der(19)t(13;19)(q21;p13)	M14	m7	<i>m16</i>	m4	m9	mM	m4	<i>m16</i>		m3	m6	m5	<i>m9</i>
i(20)(q10)	M15	19	m11?					m11?					
der(22)t(8;22)(q24;q13)	M16	m10	m10	m16	m24	mT				m10	m10	m17	<i>m13</i>
der(13;13)(q10;q10)del(13)(q12)del(13)(q14)	M17			m6?									
der(15;21)(q10;q10)	M18												
del(7)(p21)	M19		m9										
der(7)t(3;7)(p21;p21)	M20												
der(4;15)(q10;q10)	M21												
der(5;9)(p10;p10)	M22	m9b								m9	m9	m7	<i>m12</i>
i(9)(p10)	M23		m14										
17ps	M24												
der(1;21)(q10;q10)	M25												
der(3)t(3;9)(q25?;q34?)del(3)(p21?)	M26												
der(5;5)(p10;p10)t(5;22)(p15?;q13?)	M27												
del(13)(q13)	M28												
der(13;19)(q10;p10)	M29												
18ps	M30												
i(20)(p10)	M31												
N ^a	31	17	16	15	15	14	6	7	5	6	6	6	6

^a Total number of markers listed in a column.

clonal marker (M9) containing 16p. As expected, CGH showed a balance for 16q and a gain for 16p.

Chromosome 17 was commonly present as four normal copies; therefore, CGH should display a copy number gain. However, only a slight increase in copy number gain was detected, suggesting that tetraploidy for this chromosome was not present in >50% of the cell population. Previous G-banding studies have usually identified three chromosomes 17.

Two or three normal copies of chromosomes 18 were present in HeLa. CGH showed a slight loss of 18, reflecting the loss of 18 in a subpopulation of cells.

Chromosome 19 was represented by two normals and two clonal markers (M8 and M14). In M8, a small piece of 19 was present, as confirmed with conventional FISH, but its band origin remained elusive. Because M14 contained 19p13→qter and CGH is balanced for 19, the unknown piece of M8 possibly originated from 19p13→qter.

Chromosome 20 was present as two normals and two clonal markers (M5 and M15). M5 contained chromosome arm 20q, and M15 was an isochromosome 20q, resulting in a total of five copies of 20q and two for 20p. CGH showed a gain of 20q and a loss of 20p.

Subclone A usually contained three normal chromosomes 21 and no clonal markers. Subclone B contained two normals and one subclone B-specific marker (M18), which was a Robertsonian translocation, der(15;21). The total copy number of chromosome 21 equaled 3, and CGH showed a balanced ratio profile.

Chromosome 22 was present as two normal copies and two clonal markers (M6 and M16). M6 was a complex unbalanced translocation

involving chromosomes 5, 8, and 22 and contained 22q11→q13, and M16 was a der(22)t(8; 22) with the breakpoint in 22q13 as well. Conventional FISH confirmed the presence of chromosome 22 material in both markers (data not shown). On the basis of SKY, a copy number gain was expected for 22q11→q13 and a copy number loss for 22q13→qter. However, CGH showed a balance for this region, which might be due to the limited spatial resolution of CGH.

Chromosomes 6, 10, 14, and X each had three normal copies and were not involved in clonal markers. Accordingly, the CGH ratio value was $r = 1$.

FISH Localization of HPV18 Integration Sites. We detected HPV18 sequences by FISH on chromosome 8 and two abnormal chromosomes identified previously as derivatives 5 and 22. These results were consistent with radioactive ISH analyses (3). The derivation of these two aberrant chromosomes has been resolved by SKY (Table 1). Both markers contained material from chromosome 8, and CGH displayed a gain of region 8q24→qter. HeLa chromosomes were cohybridized with HPV18 and *c-MYC* probes to determine the copy number of these genes. Fifty complete metaphases were analyzed and in all of the spreads; HPV18 and *c-MYC* signals were detected at five sites as closely spaced or overlapping signals (Fig. 3A). On the basis of the size of the fluorescence hybridization signals, we estimated 5–10 copies of HPV18 per integration site. The HPV18 and *c-MYC* hybridization signals were inseparable in interphase nuclei with diffuse and relatively decondensed chromatin as well as in prophase and prometaphase nuclei. Colocalization was detected in 8q24 on three normal chromosomes 8 and at the distal end of the p arm of M6 and the distal end of the q arm of M16, where the chromosome 8 material

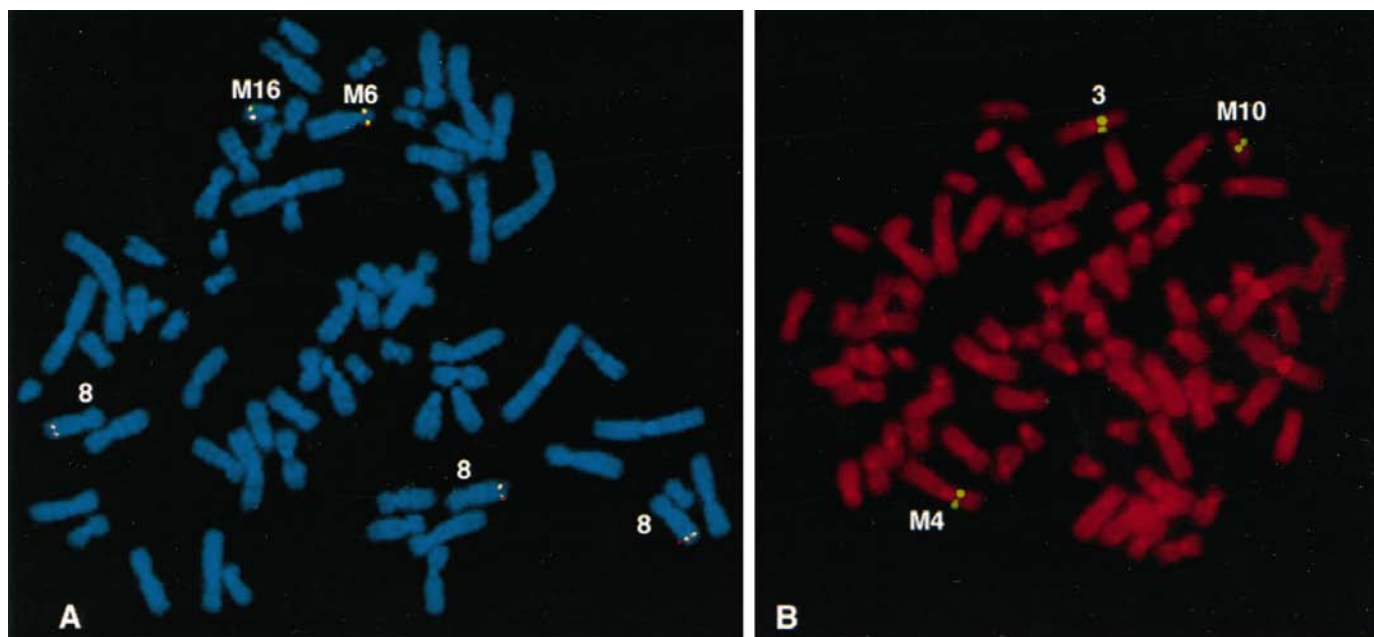


Fig. 3. A, the HPV18 (FITC, green) and *c-MYC* (TRITC, red) fluorescent signals that colocalized (yellow) on HeLa metaphase chromosomes (DAPI, blue) on normal chromosomes 8 at 8q24 and on two abnormal chromosomes, M6 and M16, now known to contain chromosome band 8q24 as well. B, HeLa metaphase chromosomes (propidium iodide, red) with the *FHIT/FRA3B* locus-specific FISH signals (FITC, yellow) mapping to 3p14.2 on one normal chromosome 3 and two abnormal chromosomes, M4 and M10.

was located in both markers. The presence of *c-MYC* in M6 and M16 confirmed the presence of 8q24.

HeLa Karyotype Comparison. We have compared the HeLa spectral karyotype with karyotypes published previously that were analyzed by G-banding (2, 4, 6–11) and FISH (12). Table 3 shows 31 HeLa markers characterized in this study. In our comparison, we chose to avoid karyotypes of different sublines and variations of HeLa, HeLa-like cell lines, and HeLa-contaminated cell lines. Nevertheless, a comparison with HeLa S3 and HeLa-variation D98/AH-2 was made for historical perspective.

The genome of HeLa has remained stable after decades of weekly subculturing. We found that 18 of 20 clonal markers (M1–M17 and M19) described by SKY were present in G-banding studies published previously. Two markers (M18 and M20) were not noticed or were not present before. Six of the 18 markers (M1, M2, M4, M7, M13, and M14) were described in the same way in at least one previous study, whereas 12 markers (M3, M5, M6, M8, M9, M10, M11, M12, M15, M16, M19, and M20) were identified in part or not at all. SKY and additional molecular cytogenetic techniques have fully identified these markers. One of the 12, M8 der(7)t(7;19)(q35;p13), was never recognized as being aberrant in the G-banding karyotypes. M8 was possibly present in three studies (6, 8, 9) but classified as a normal seven instead. M6 der(5)t(5;8;22) was recognized as being aberrant only by Popescu *et al.* (3, 6) and Chen (2); in all other reports, it was classified as a normal chromosome 5. Markers M22 and M23 were present in previous G-banding (2, 6) studies and may, therefore, be of clonal origin. M22 was identified in D98/AH-2 by FISH (12). Nelson-Rees *et al.* (10) have given the description of markers found in HeLa CCL2 and HeLa S3 but did not show a full karyotype with the normal chromosomes. Therefore, there might be more common markers present than the six (CCL2) and five (S3) listed in Table 3. We found that HeLa CCL2 had six markers in common with D98/AH-2, which was studied by FISH with chromosome painting libraries (12) and G-banding (4, 8, 11). The discrepancies between our study and FISH whole-chromosome painting by Ruess *et al.* (12) merely exist because D98/AH-2 is a subline that is cytogenetically different from HeLa CCL2.

DISCUSSION

The definitive karyotype of HeLa was resolved by combining the molecular cytogenetic techniques SKY, CGH, and FISH. The origins of all complex rearrangements previously unidentified in G-banding studies have been resolved. Comparison with previous G-banding studies revealed HeLa to be remarkably stable after years of cultivation because 18 of 20 clonal markers found in HeLa were present in earlier studies (Table 3).

SKY and CGH analyses together have unprecedented power for resolving structural and numerical chromosomal aberrations. Twenty-four-color FISH analysis by SKY readily identifies the origins of rearranged chromosomes. When uncertainty remained after SKY about the origin of subtle translocated regions *e.g.*, at a telomeric end or regions spanning less than one chromosome band, conventional FISH was used to establish the origin by using a flow-sorted whole chromosome painting probe. In this study, all confirmation experiments verified the initial identification of chromosomal material based on SKY. Alignment of the SKY-classified chromosomes with the companion inverted DAPI banding image was used to identify the chromosome band regions. Although the inverted gray-scale images of high quality DAPI-stained chromosomes were similar to G-banding, the banding resolution of HeLa metaphases in this study were sometimes suboptimal, making accurate breakpoint mapping difficult. CGH maps overall chromosomal copy number changes (gains and losses) of the tumor DNA over the length of the chromosome. In principal, therefore, any clonal aberration that causes a numerical imbalance is detected by CGH. In the few instances where SKY and inverted DAPI banding analysis were unsuccessful in identifying the origin of the chromosomal material involved, the CGH copy number change was indicative. A clear example of karyotype refinement by CGH was demonstrated for M3 dup(2q), where the extra material was determined to originate from the gained region in CGH, 2q31→q36. There is striking similarity between the SKY amplification-deletion map and the CGH ratio profile, considering that the SKY analysis was based on 24 metaphase cells, whereas CGH analysis was based on DNA extracted from millions of cells. The clonal aberrations as

described by SKY in the two subclones are representative for the entire HeLa population. This view was strengthened because 18 of 20 markers identified by SKY were present in the G-banding studies reported more than 10 years ago (Table 3).

Balanced translocations, as detected frequently in hematological malignancies, were not identified in HeLa cells. Gain of function of proto-oncogenes and loss of function of tumor suppressor genes is mostly achieved via copy number changes that are detectable cytogenetically. Of course, activation or inactivation by point mutations remains elusive. The gain of chromosome arm 5p was mapped frequently in advanced stage cervical squamous cell carcinomas (29) and in other cell lines established from cervical cancers.⁵ SKY analysis of HeLa chromosomes identified the formation of three to five isochromosomes 5p as one of the underlying cytogenetic mechanisms by which chromosome arm copy number increases are acquired. The amplification of the entire short arm of chromosome 5 suggests the presence of genes whose gain of function seems to be highly advantageous in advanced stage cervical carcinomas and in cervical carcinoma cell lines.

In a relatively limited number of cases of cervical carcinoma cell lines or tumor samples examined, HPV was found integrated at apparently normal chromosomal sites (30). In contrast, current FISH analysis demonstrated colocalization of HPV18 and *c-MYC* sequences in two rearranged sites. This strongly indicates genomic reorganization caused by the viral insertion and is consistent with a statistical analysis showing a correlation between the breakpoints in structural rearrangements and HPV sites of integration in cervical carcinomas (31).

The complex marker M11 was present in all previous G-banding studies (Table 3) but has never been fully described before. SKY and additional FISH using chromosome painting probes for chromosomes 9 and 11 and *c-ABL1*-specific probes revealed M11 to contain chromosome 11 material and 9q34 segments on both distal ends. The HPV18 integration at 9q34 (3) was not confirmed in this study. The exact rearrangement of chromosome 11 segments in M11 could not be derived from SKY, FISH, or conventional cytogenetic techniques in this study. CGH analysis suggested, however, a deletion of 11q23→qter, possible deletion of 11p15→pter, and amplification of 11p14→p11 and 11q13→11q22. HeLa furthermore contained two normal chromosomes 11. On the basis of chromosome microcell transfer studies of chromosome 11 into HeLa cells (32), it has been suggested that chromosome 11 contains tumor suppressor genes. LOH studies on cervical cancer localized a putative site to 11q22→q24 (33). This is in accordance with our CGH findings showing loss of 11q23→qter. Additional FISH for chromosome band 11q13, containing the *cyclin D1* gene, is necessary to elucidate presence of this region in HeLa because this region has been found to be involved in multiple translocations in HeLa sublines such as DH98/AH-2 (34, 35).

In conclusion, we reported here the most complete chromosomal characterization of the HeLa cervical cancer cell line. Numerical and structural chromosomal aberrations identified by SKY and inverted DAPI banding analysis, genomic imbalances detected by CGH as well as FISH localization of HPV18 integration at a fragile site and *c-MYC* locus in HeLa cells are common and representative for advanced stage cervix squamous carcinomas (29, 36, 37). Thus, genomic alterations in HeLa cells are highly relevant to the pathology of cervical neoplasia and provide a reference for future studies in cervical cancer.

ACKNOWLEDGMENTS

We thank Dr. S. du Manoir and Dr. K. Heselmeyer-Haddad (Genome Technology Branch, National Human Genome Research Institute, NIH, Bethesda, MD) for assistance with CGH analysis and helpful discussions; M. van der Linden and D. Laferty (Leica Imaging, Cambridge, United Kingdom) for adapting QFISH image acquisition to CGH; and M. Gregson (Applied Imaging, Cambridge, United Kingdom) for implementing Cy5 display into Cytovision 3.0 CGH analysis software. Image acquisition and analyses software was developed under NIH-CRADA terms with Applied Spectral Imaging, Ltd., Applied Imaging, Ltd., and Leica Imaging Systems, Ltd.

REFERENCES

- Gey, G. O., Coffman, W. D., and Kubicek, M. T. Tissue culture studies of the proliferative capacity of cervical carcinoma and normal epithelium. *Cancer Res.*, *12*: 264–265, 1952.
- Chen, T. R. Re-evaluation of HeLa, HeLa S3, and HEP-2 karyotypes. *Cytogenet. Cell Genet.*, *48*: 19–24, 1988.
- Popescu, N. C., DiPaolo, J. A., and Amsbaugh, S. C. Integration sites of human papillomavirus 18 DNA sequences on HeLa cell chromosomes. *Cytogenet. Cell Genet.*, *44*: 58–62, 1987.
- Stanbridge, E. J., Flandermeier, R. R., Daniels, D. W., and Nelson-Rees, W. A. Specific chromosome loss associated with the expression of tumorigenicity in human cell hybrids. *Somatic Cell Genet.*, *7*: 699–712, 1981.
- Lichy, J. H., Modi, W. S., Seanez, H. N., and Howell, P. M. Identification of a human chromosome 11 gene which is differentially regulated in tumorigenic and non-tumorigenic somatic cell hybrids of HeLa cells. *Cell Growth Differ.*, *3*: 541–548, 1992.
- Popescu, N. C., and DiPaolo, J. A. Preferential sites for viral integration on mammalian genome. *Cancer Genet. Cytogenet.*, *42*: 157–171, 1989.
- Mincheva, A., Gissman, L., and Zur Hausen, H. Chromosomal integration sites of human papillomavirus DNA in three cervical cell lines mapped by *in situ* hybridization. *Med. Microbiol. Immunol.*, *176*: 245–256, 1987.
- Heneen, W. K. HeLa cells and their possible contamination of other cells: karyotype studies. *Hereditas*, *82*: 217–248, 1976.
- Kraemer, P. M., Deaven, L. L., Crissman, H. A., Steinkamp, J. A., and Petersen, D. F. On the nature of heteroploidy. *Cold Spring Harb. Symp. Quant. Biol.*, *38*: 133–144, 1973.
- Nelson-Rees, W. A., Hunter, L., Darlington, G. J., and O'Brien, S. J. Characteristics of HeLa strains: permanent vs. variable features. *Cytogenet. Cell Genet.*, *27*: 216–231, 1980.
- Francke, U., Hammond, D. S., and Schneider, J. A. The band patterns of twelve D98/AH-2 marker chromosomes and their use for identification of intraspecific cell hybrids. *Chromosoma (Berl.)*, *41*: 111–121, 1973.
- Ruess, D., Ye, L., and Grond-Ginsbach, C. HeLa D98/AH-2 studied by chromosome painting and conventional cytogenetic techniques. *Chromosoma (Berl.)*, *102*: 473–477, 1993.
- Speicher, M. R., Ballard, S. G., and Ward, D. C. Karyotyping human chromosomes by combinatorial multi-fluor FISH. *Nat. Genet.*, *12*: 368–375, 1996.
- Schröck, E., du Manoir, S., Veldman, T., Schoell, B., Wienberg, J., Ferguson-Smith, M. A., Ning, Y., Ledbetter, D. H., Bar-Am, I., Soenksen, D., Garini, Y., and Ried, T. Multicolor spectral karyotyping of human chromosomes. *Science (Washington DC)*, *273*: 494–497, 1996.
- Garini, Y., Macville, M., du Manoir, S., Buckwald, R. A., Lavi, M., Katzir, N., Wine, D., Bar-Am, I., Schröck, E., Cabib, D., and Ried, T. Spectral karyotyping. *Bioimaging*, *4*: 65–72, 1996.
- Kallioniemi, A., Kallioniemi, O., Sudar, D., Rutovitz, D., Gray, J. W., Waldman, F., and Pinkel, D. Comparative genomic hybridization for molecular cytogenetic analysis of solid tumors. *Science (Washington DC)*, *258*: 818–821, 1992.
- Zimonjic, D. B., and Popescu, N. C. An improved procedure for chromosome preparations from solid tumors. *Cancer Genet. Cytogenet.*, *72*: 161, 1994.
- Macville, M., Veldman, T., Padilla-Nash, H., Wangsa, D., O'Brien, P., Schröck, E., and Ried, T. Spectral karyotyping, a 24-colour FISH technique for the analysis of chromosomal rearrangements. *Histochem. Cell Biol.*, *108*: 299–305, 1997.
- Telenius, H., Pelmeur, A. H., Tunnacliffe, A., Carter, N. P., Behmel, A., Ferguson-Smith, M. A., Nordenskjöld, M., Pfragner, R., and Ponder, B. A. J. Cytogenetic analysis by chromosome painting using DOP-PCR amplified flow-sorted chromosomes. *Genes Chromosomes Cancer*, *4*: 267–270, 1992.
- Malik, Z., Dishi, M., and Garini, Y. Fourier transform multipixel spectroscopy and spectral imaging of protoporphyrin in single melanoma cells. *Photochem. Photobiol.*, *63*: 608–614, 1996.
- Mitelman, F. (ed.). *ISCN: An International System for Human Cytogenetic Nomenclature*. Basel: S. Karger, 1995.
- Sambrook, J., Fritsch E. F., and Maniatis, T. (eds.). *Molecular Cloning: A Laboratory Manual*. Cold Spring Harbor, NY: Cold Spring Harbor Laboratory, 1989.
- du Manoir, S., Speicher, M. R., Joos, S., Schröck, E., Popp, S., Döhner, H., Kovacs, G., Robert-Nicoud, M., Lichter, P., and Cremer, T. Detection of complete and partial chromosome gains and losses by comparative genomic *in situ* hybridization. *Hum. Genet.*, *90*: 590–610, 1993.
- Dunham, I., Lengauer, C., Cremer, T., and Featherstone, T. Rapid generation of chromosome specific alphoid DNA probes using the polymerase chain reaction. *Hum. Genet.*, *88*: 457–462, 1992.

⁵ M. Macville *et al.*, manuscript in preparation.

25. Ried, T., Petersen, I., Holtgreve-Grez, H., Speicher, M. R., Schröck, E., du Manoir, S., and Cremer, T. Mapping of multiple DNA gains and losses in primary small cell lung carcinomas by comparative genomic hybridization. *Cancer Res.*, *54*: 1801–1806, 1994.
26. Ohta, M., Inoue, H., Cotticelli, M. G., Kastury, K., Baffa, R., Palazzo, J., Siprashvili, Z., Mori, M., McCue, P., Druck, T., Croce, C., and Huebner, K. The *FHIT* gene, spanning the chromosome 3p14.2 fragile site and renal carcinoma-associated t(3;8) breakpoint, is abnormal in digestive tract cancers. *Cell*, *84*: 587–597, 1996.
27. Zimonjic, D. B., Druck, T., Ohta, M., Kastury, K., Croce, C., Popescu, N. C., and Huebner, K. Position of chromosome 3p14.2 fragile site (FRA3B) within the *FHIT* gene. *Cancer Res.*, *57*: 1166–1170, 1997.
28. Zimonjic, D. B., Simpson, S., Popescu, N. C., and DiPaolo, J. A. Molecular cytogenetics of human papilloma virus-negative cervical carcinoma cell lines. *Cancer Genet. Cytogenet.*, *82*: 1–8, 1995.
29. Heselmeyer, K., Macville, M., Schröck, E., Blegen, H., Hellström, A.-C., Shah, K., Auer, G., and Ried, T. Advanced stage cervical carcinomas are defined by a recurrent pattern of chromosomal aberrations revealing high genetic instability and a consistent gain of chromosome 3q. *Genes Chromosomes & Cancer*, *19*: 233–240, 1997.
30. Popescu, N. C. Chromosome fragility and instability in human cancer. *Crit. Rev. Oncol.*, *5*: 121–140, 1994.
31. De Braekeleer, M., Sreekantaiah, C., and Haas, O. Herpes simplex virus and human papillomavirus sites correlate with chromosomal breakpoints in human cervical cancer. *Cancer Genet. Cytogenet.*, *59*: 135–137, 1992.
32. Saxon, P. J., Srivatsan, E. S., and Stanbridge, E. J. Introduction of human chromosome 11 via microcell transfer controls tumorigenic expression of HeLa cells. *EMBO J.*, *5*: 3461–3466, 1986.
33. Hampton, G. M., Penny, L. A., Baergen, R. N., Larson, A., Brewer, C., Liao, S., and Busby-Earle, R. M. C. Loss of heterozygosity in cervical carcinoma: subchromosomal localization of a putative tumor-suppressor gene to chromosome 11q22–24. *Proc. Natl. Acad. Sci. USA*, *91*: 6953–6957, 1994.
34. Misra, B. S., and Srivatsan, E. S. Localization of HeLa cell tumor-suppressor gene to the long arm of chromosome 11. *Am. J. Hum. Genet.*, *45*: 565–577, 1989.
35. Jesudasan, R. A., Slovak, M. L., Sen, S., and Srivatsan, E. S. Rearrangement of chromosome band 11q13 in HeLa cells. *Anticancer Res.*, *14*: 1727–1734, 1994.
36. Popescu, N. C., and DiPaolo, J. A. Cytogenetics of cervical neoplasia. *Cancer Genet. Cytogenet.*, *60*: 214–215, 1992.
37. Atkin, N. B. Cytogenetics of carcinoma of the cervix uteri: a review. *Cancer Genet. Cytogenet.*, *95*: 33–39, 1997.